Fracture of Ceramic Materials under Dynamic Loadings

E.G. Skripnyak, V.V. Skripnyak, V.A. Skripnyak, and I.K. Vaganova

Tomsk State University, Department of Mechanics of Solids

36 Lenin Avenue, Tomsk, Russia, 634050,

skrp@ftf.tsu.ru

Keywords: Mechanical properties, nanostructured ceramics, dynamic loading, fracture.

Abstract. Results of experimental and theoretical investigations of the influence of voids structure, grains structure and phase structure on mechanical properties of Al_2O_3, ZrO_2, and ceramic composites $Al_2O_3 - ZrO_2 - Y_2O_3 - MgO$ under dynamic loading are presented in the given work. Deformation and damage of structured representative volumes of ceramic materials on meso-scale level were simulated under quasistatic and shock wave loadings. The critical fracture stress on meso-scale level depends not only on relative volumes of voids and strengthened phases, but also sizes of corresponding structure elements. At identical porosity, concentration of nano-voids near grain boundaries causes the decreasing of the shear strength of nanostructured and ultrafine-grained ceramics.

Introduction

The prediction of fragmentation of modern ceramic materials under dynamic loadings is the complicated problem owing to insufficient knowledge about laws of structure evolution and nucleation and accumulation of damages. Studies on the deformation and fracture laws pertaining to materials subjected to intense dynamic loading are among the hottest areas of research into the physics of condensed matter. Of particular interest are investigations into the deformation and fracture processes developing in nanostructured ceramics under pulsed and shock loading [1-4]. These investigations provide information on the fundamental strength properties of the materials. Shock waves enable peculiar states characterized by high internal-energy densities to be produced in the media. In these conditions, nucleation of defects, activation of localized-deformation bands and microcracks dispersed in an elementary volume of the material, and self-organization processes are observed in the ceramic structure. Interest in the problems of relevance for the present discussion has quickened after the discovery of failure waves in silicon oxide and soda lime glass [5].

At present considerable study is being given to the mechanisms of dynamic fracture operative in oxide nanoceramics. Nanoceramics are commonly referred to as the class of materials whose average grain size is less than several tens of nano-meters. The microstructure of oxide nanoceramics consists of several condensed phases and porosity Shock-wave amplitudes in the gigapascal range are found to bring about structural changes in Al_2O_3, $ZrO_2–Y_2O_3$ nanoceramics, resulting in a substantial falling of the strength of the materials [2, 6 - 7]. The damage was observed not only in a spalling region where transient tensile stresses are in operation, but also in a material zone experiencing shock-wave compression. Local failure of the ceramics in condensed phase may be favored by micro-void structure as well. The fracture mechanisms at work in porous nanoceramics under dynamic loading are still understood incompletely. In the present work, this approach has been adopted to investigate the mechanisms involved in the deformation and damage accumulation in porous oxide nanoceramics structure under shock loading.

We have investigated the damage mechanisms operative in a representative structured volume of porous nanoceramics at homologous temperatures $T/T_m < 0.1$ under shock wave amplitudes above the Hugoniot elastic limit (HEL). Fig.1 shows a voids structure and grain structure for Al_2O_3 nanoceramics. The voids size far exceeds the average grain size in condensed phase, and the voids display spatial distribution over the volume of the material. Histograms of grain size and void size distributions for the specimen of Al_2O_3 ceramics are shown in Fig.2.

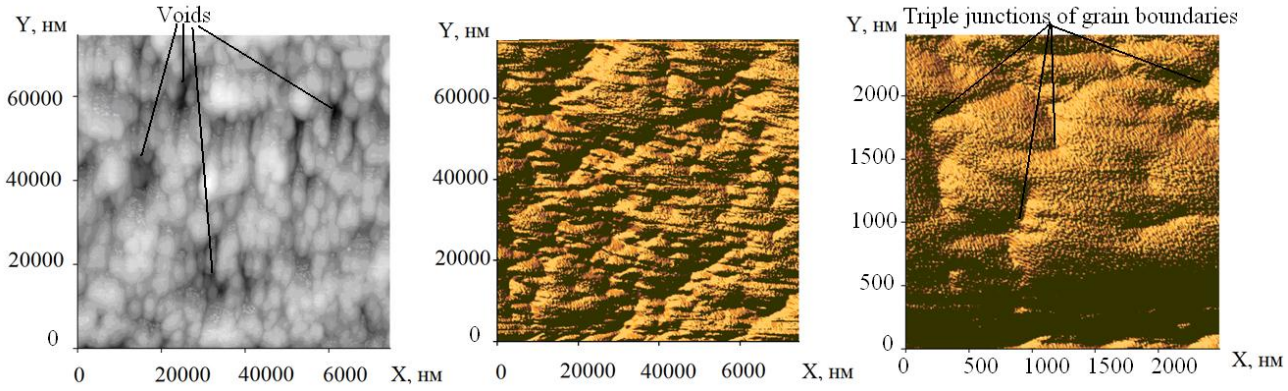

Fig.1. Grain and micro-void structure of Al_20_3-1,5 vol. % MgO ceramics.

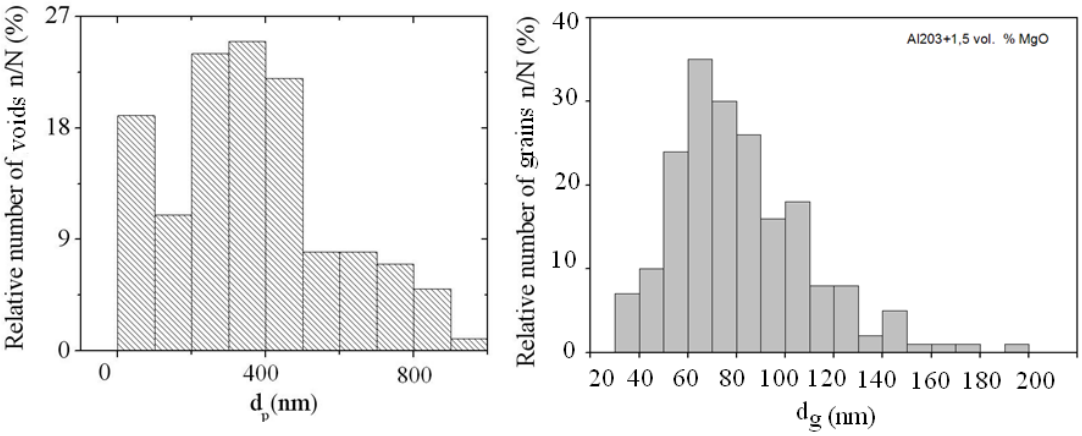

Fig. 2. Histograms of grain size and void size distributions for the specimen of Al_2O_3 ceramics.

The representative volume element (RVE) of porous nanoceramics are generated for a given voids size distribution d_p, relative void volumes a, and void shape factor ϑ.

The used method allows creating a model porous structure in RVE of a ceramic material for a 3-D problem. Models of the RVE of nanoceramics containing the isolated voids and clusters of voids are displayed in Fig. 3a and Fig. 3b respectively. Dimensions of RVE are 5 μm $\times 5$ μm $\times 5$ μm. The porosity of both this RVE is equal to 4.3 %. The voids are surrounded by a condensed phase exhibiting the properties of condensed phase nanocrystalline oxide ceramics. The deformation of condensed phase is described by means of an approach adopted in the mechanics of damaged media [1-4,8]. Consider a volume of porous nanoceramics under plane-wave loading (see Fig.3c). The kinematics of the medium in condensed phase is described by strain tensor and rotation tensor components. In the Lagrangian reference the system of equations includes conservation equations of mass, momentum, and energy, constitutive equations, and equation of the damage parameter evolution. In condensed phase the pressure up to 10 GPa is calculated by the Mie-Grüneisen equation of states. Condensed phase of oxide ceramics under deformation may exhibit micro-crack

nucleation [1–7]. As this takes place, the shear strength of the elementary volume of the material containing cracks is decreased.

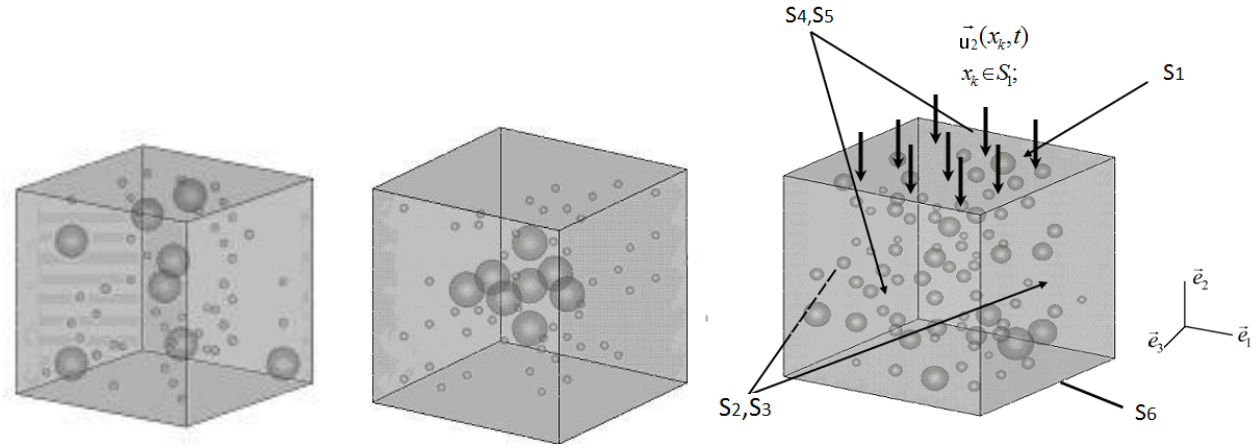

Fig. 3. Model RVE of porous nanoceramics.

To account for loss in the local shear strength of the elementary volume, we have introduced the damage parameter D for the medium [1,8]. Equation (1) is offered for description of D evolution under dynamic fracture of nanostructured oxide ceramic by a model of microcracks nucleation and growth.

$$\begin{aligned} D &= D \qquad\qquad if \qquad D \le D^*, \\ D &= D^* + K(D - D^*) \; if \qquad D > D^*, \end{aligned} \tag{1}$$

where $D^* \approx 0{,}2$ is the percolation limit of damages, K is the factor of a material considering voids morphology.

$$D = \sum_{k=0} [\Delta \varepsilon_{eq}{}^{p} / \varepsilon_f]_k, \quad , \qquad D = 1 \quad if \quad \sigma_1 \le -\sigma_f, \tag{2}$$

where $[\Delta \varepsilon^p]_k = \int_{t_k}^{t_{k+1}} \dot{\varepsilon}_{eq}^{p} \, dt$, $\dot{\varepsilon}_{eq}^{p}$ is the equivalent inelastic strain rate, and ε_f is the strain for which the elementary volume is fragmented due to the cracking effect,

$$\varepsilon_f = D_1 (P^* + T^*)^{D_2}, \tag{3}$$

$$\sigma_s^c = A_1 (P^* + T^*)^{m_1} (1 + C_1 \ln \dot{\varepsilon}), \tag{4}$$

$$\sigma_f = B_2 (P^*)^{m_2} (1 + C_2 \ln \dot{\varepsilon}) \; . \tag{5}$$

Here A_1, B_2, C_1, C_2, D_1, D_2, m_1, and m_2 are material parameters,
$\dot{\varepsilon} = \dot{\varepsilon} eq / \dot{\varepsilon}_0$, $\dot{\varepsilon}_0 = 1 [s^{-1}]$ is the normalized inelastic equivalent strain rate,
$T^* = (T - T_r) / (T_m - T_r)$, T_m is the melting temperature, $T_r = 293$ K,
$P^* = P/P_{HEL}$, P_{HEL} is the pressure corresponding to the HEL.
In the case of no cracks in condensed phase in the initial state, the damage parameter is zero.
The stress deviator tensor is calculated in the framework of the Drukker-Prager model and Eq.(4).

For instance, in Al_2O_3 in condensed phase, the following values of the coefficients were used: $\rho_0 =$ 3.96 g/cm^3, D_1 = 0.001, D_2 = 1, P_{HEL} = 5.85 GPa, A = 5.14 GPa, C= 0, m = 0.6.

Fragmentation process of material at meso-scale level was described by model of fractal clusters generation. Formation of the neighbors of fractured material micro-volumes cells with damage parameter D=1 considered as element cluster. It was supposed that fracture of micro-volume cells are irreversible. Effective size of fractured cells fractal cluster was calculated by the formula

$$R_{ij} = \sum_{k=1}^{M} (x_{ki} - x_{kj})^2 \ , \tag{6}$$

where M is a total number of cells in RVE, x_{ki} is coordinate of a fractured cell.

$$\lambda_j = \sum_{i=1}^{N} \Delta R_{ij} \tag{7}$$

As criterion of RVE fracture corresponds to full loss of the shear strength is

$$\lambda_j \geq N_{\lambda j}, \tag{8}$$

where $N_{\lambda j}$ is the minimum number of cells in a probable fracture surface in RVE, j is component of normal vector to fracture surface.

Average value of D calculated by formula

$$D_{ave} = \sum_{i=1}^{n} D_i / n, \tag{9}$$

where n is a number of damaged material particles in RVE.

RESULTS AND DISCUSSION

Fig. 4 shows variations of the damage parameter in model RVEs (Fig. 3a,b) in the wake of the front of the elastic wave precursor.

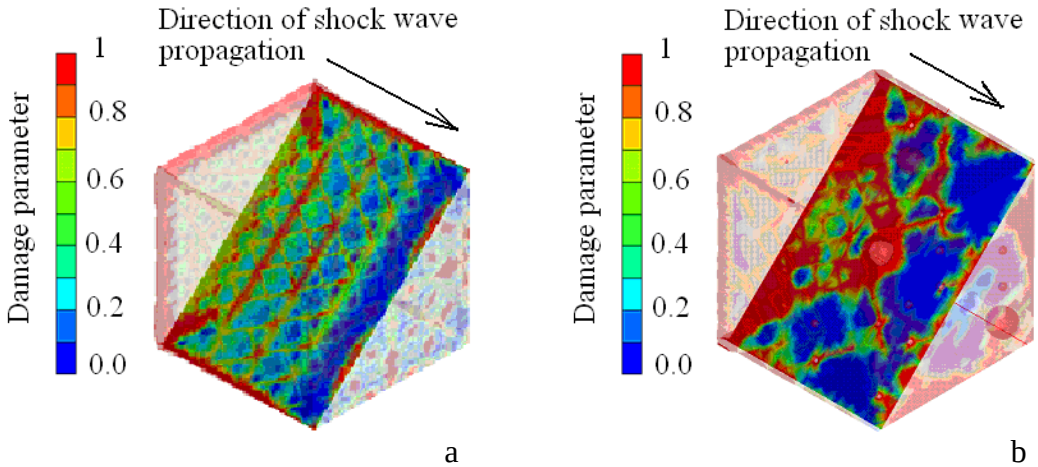

a b

Fig. 4. Damage parameter distribution in a model volume of porous nanoceramics.

Fig 4b shows distribution of damage parameter in a model volume of nanoceramics with clusters of voids. Damage accumulation and fragmentation occur in different compression stages in condensed phase. Within the elastic wave precursor, the pore shape and size are not subjected to substantial changes. The average velocity of propagation of the elastic precursor in porous ceramics is lower

than in condensed phase. The decrease in the average elastic precursor velocity is due to the interaction of the wave front with the pore surface. Collapse of voids in the bulk compression wave is due to the displacement of fragments of the fractured material in condensed phase toward voids. The thickness of the fragmentation zones around pores is greater than the initial average pore size.

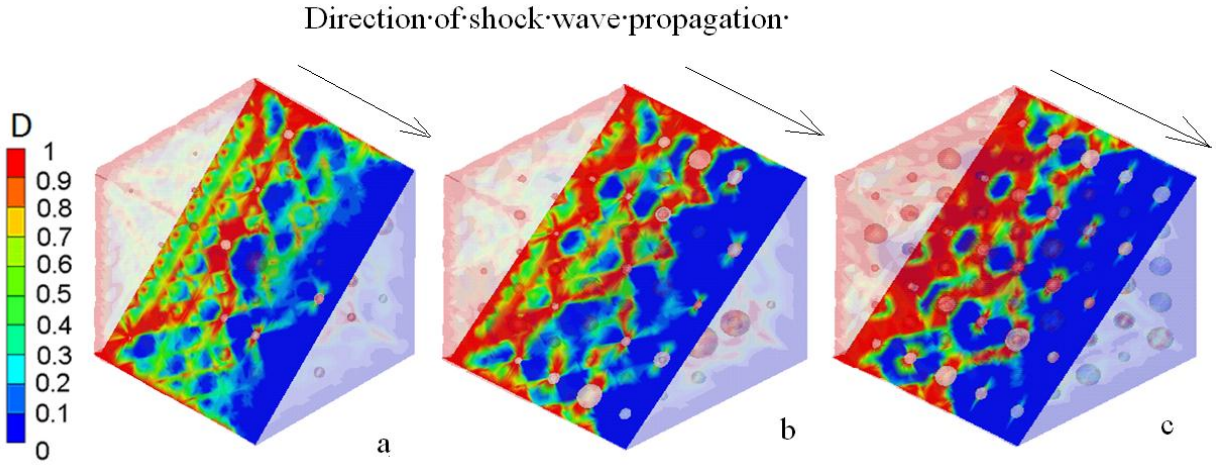

Fig. 5. Fragmentation of porous Al_2O_3 nanoceramics behind of shock wave.

Fig. 5 shows the distribution of damage parameter D at the moment of time 0,045μs in model RVEs of porous Al_2O_3 with behind a shock wave with amplitude of 7,5 GPa. It is evident from Fig. 5 that variations of the voids distribution in RVE occur with a dramatic increase in damaging the material in condensed phase seen in narrow extended zones. The damage zones are oriented for the most part along, across, and at an angle of ~ 45º to the direction of propagation of the shock wave. The fracture spots of transverse orientation are primarily observed near voids. The pores are transformed from a spherical to an ellipsoidal and, finally, to a circular (disk-like) shape within the wave front under the effect of hydrostatic pressure. The alteration of the voids shape causes the stress concentration to increase in the plane orthogonal to the direction of propagation of the shock wave.
Local pressure relaxation near pores gives rise to gradients of the particle velocity components in the direction orthogonal to that of propagation of the shock wave. This results in generation of damage zones running parallel to the direction of propagation of the wave. The final stage of fragmentation of the material in condensed phase is connected with shift and turn of the blocks with the damage zones in between. The fragment size in porous ceramics under shock loading (Fig. 5) may differ essentially. The average fragment size is smaller than the spacing between pores, L_p.

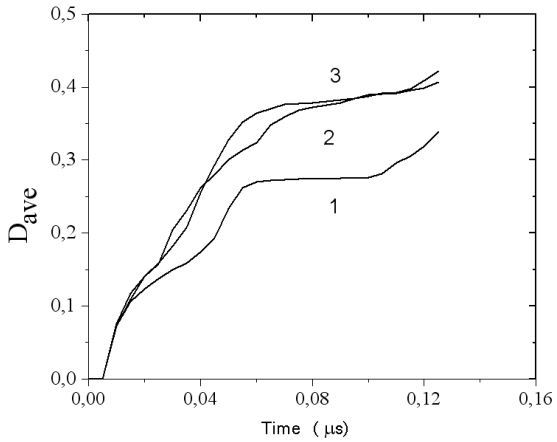

Fig. 6. Average damage parameter D_{ave} versus time under compression in shock wave.

Fig. 6 shows kinetics of averaged damage parameter D_{ave} for models of Al_2O_3 ceramics with 3 types of void sizes distributions under shock wave loading with amplitude of 7,5 GPa. Average sizes of voids were equal to 30, 39, and 40 nm for curves 1, 2, 3 correspondingly. The number of voids was assumed identical in examined models of RVE. The averaged porosity of models 1, 2, 3 was 0,88, 1,99, and 4,26 % correspondingly. Kinetics of damaging of porous oxide ceramics under shock pulse compression considerably depends on size of voids. Damage of oxide nanoceramics with nano-size voids is less than in ceramics with micro-size voids under pulse loading with amplitudes above the HEL.

The modeling results for shock wave propagation in nanoceramics and ceramic nanocomposites with specified microstructure make it possible to estimate the effective elastic moduli under dynamic compression. Fig.7 shows particles velocity in $Al_2O_3 - (ZrO_2 - 3\ \%\ Y_2O_3)$ nano-composite behind front of shock wave at time 6 10^{-10} s.

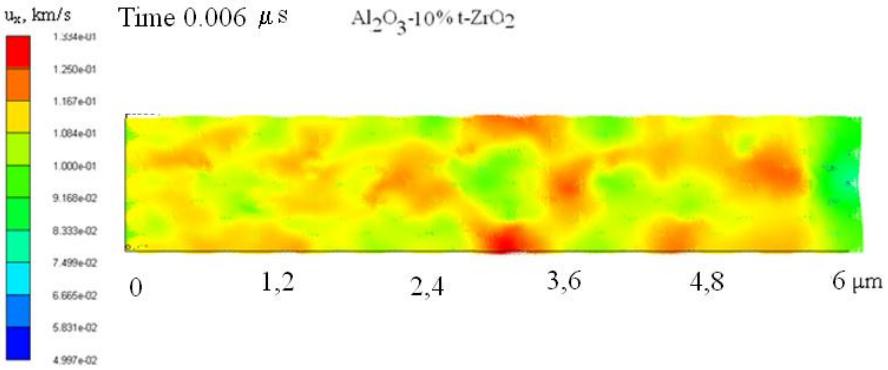

Fig.7. Particle velocities in $Al_2O_3 - 10\ \%\ (ZrO_2 - 3\ \%\ Y_2O_3)$ behind a shock wave front.

The average longitudinal elastic wave velocity C_L is found from the difference in the average distance traveled by the elastic precursor in a time Δt

$$C_L = \Delta x_1^L / \Delta t\ ,\ C_b = \Delta x_1^b / \Delta t\ . \qquad (10)$$

Here $\Delta x_1{}^L$ and $\Delta x_1{}^b$ are the distance travelled by the elastic precursor and bulk compression wave in a time Δt.

The effective Poisson ratio ν is determined by the relation

$$\nu = [3 - \xi]/[3 + \xi]\ ,\quad \xi = (C_L / C_b)^2\ . \qquad (11)$$

The effective bulk modulus K and the shear modulus μ can be estimated by relations

$$K = C_b{}^2 / \langle \rho \rangle,\ \mu = K \frac{3(1 - 2\langle \nu \rangle)}{2(1 + \langle \nu \rangle)}\ , \qquad (12)$$

where $\langle \rho \rangle = \rho_c (1 - \alpha)$, ρ_c is the condensed-phase density, α is the relative pore volume.

The method was used for estimation of C_L and C_b in Al_2O_3 and ZrO_2-3 mol % Y_2O_3 nanoceramics with 11 % porosity. For a model volume of Al_2O_3 nanoceramics, the calculated average elastic precursor velocity is 9.92 km/s, whereas the average bulk compression wave is 8.8 km/s. For ZrO_2-3 mol % Y_2O_3 the calculated average elastic precursor velocity is 6.55 km/s, and the average bulk compression wave is 5.87 km/s. Calculated values of C_L and C_b have a good correlation with

experimental data for nanoceramics with grain size from 40 to 70 nm [7]. It should be emphasized that the proposed method for estimating the effective mechanical characteristics of porous nanoceramics is applicable to material with isolated pores. Fig. 8 shows longitudinal, bulk, and the shear sound velocities versus volume concentration of strengthening phases in Al_2O_3-ZrO_2 and Al_2O_3-ZrB_2 nanocomposites.

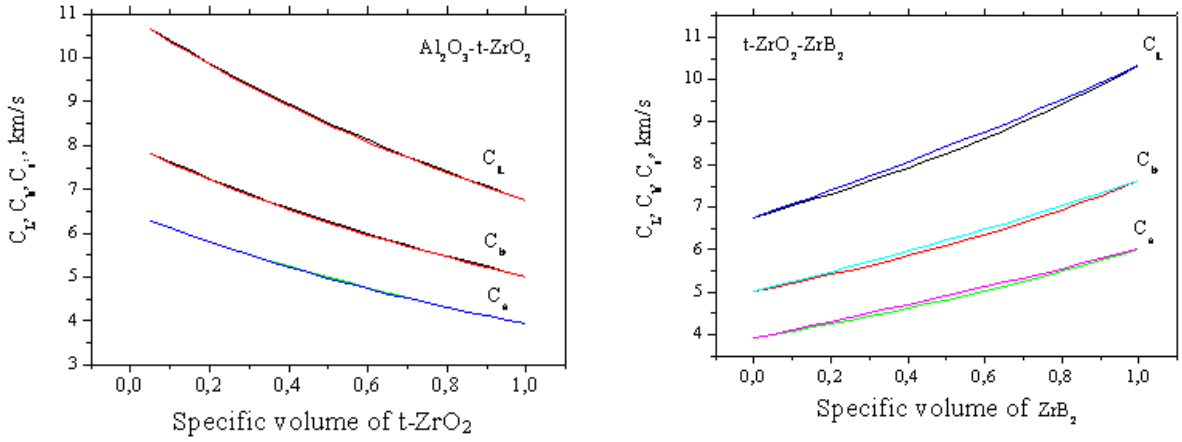

a b

Fig.8. Sound velocities versus concentration of strengthening phases.

The spall strength of ceramics and ceramic nanocomposites is strongly depends on porous structure, concentration of strengthening phase and morphological characteristics of strengthening phases. Fig. 9 shows results of simulation of spall crack formation in Al_2O_3-ZrO_2 composite under shock pulse loading. Damage of local material volumes in the spall zone lead to creation of local stress gradients within several microns far the spall crack.

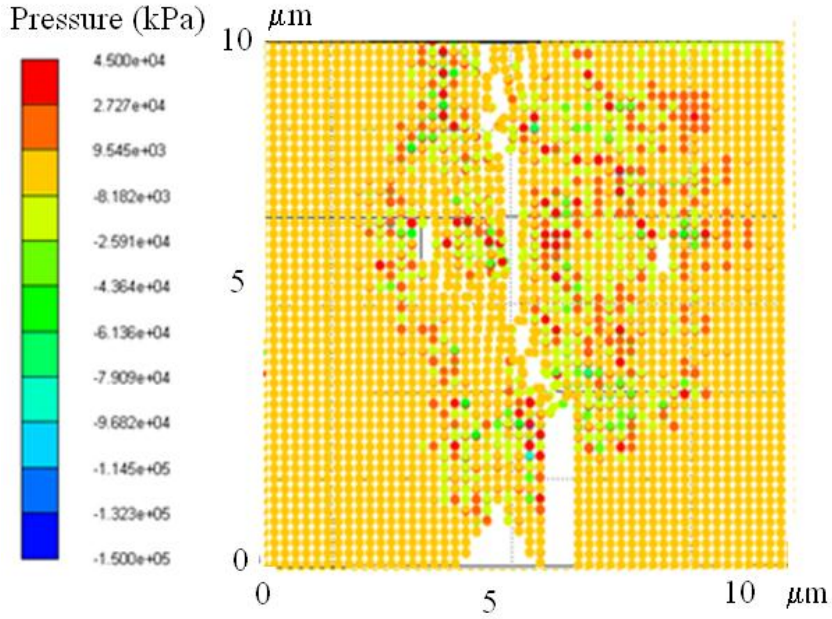

Fig. 9. Pressure distribution near the spall crack in Al_2O_3-ZrO_2 composite.

Therefore the macroscopic spall strength can be varied depending on local porous structure and strengthening phase distribution in spall zone.

Summary

The approach combining experimental methods of research of a microstructure and mechanical behavior of samples of ceramic materials at a quasistatic and dynamic loading, with the theoretical analysis and computer simulation was used in this work. Deformation and fracture of ceramic composites Al_2O_3 – t-ZrO_2 and porous ceramics under dynamic loading was investigated by computer simulation method. The model of the structured representative volume of oxide composites was developed using the data of microscopic researches.

Results of investigations have shown the dependence of damage kinetics of ceramics under dynamic loading from a concentration of nano-voids, a concentration and particles sizes of partially stabilized tetragonal phase of ZrO_2. . It was detected the macroscopic fracture is preceded by a stage of nucleation of mesocracks depending on local stress.

The presence of pores in the structure of nanoceramics makes failure wave generation difficult under dynamic loading.

Shock loading of porous nanoceramics gives rise to a system of extended zones of damaged materials oriented along, across, and at an angle of ~ 45 º to the direction of propagation of the shock wave front.

Pore structure has a profound impact on the fragment size and strength properties of oxide nanoceramics.

A method is proposed for a theoretical estimation of the effective elastic moduli of nanoceramics with pore structures.

References

[1] V.A. Skripnyak, E.G. Skripnyak, V.V. Skripnyak, and M.V. Korobenkov et. al. Izvestiya Vuzov. Fizika. (in Russian) Vol. 52, № 12 (2009), p. 46.

[2] V.A. Skripnyak, E.G. Skripnyak, and T.V. Zhukova: in Shock Compression of Condensed Matter, 2001. (M.D. Furnish, N.N. Thadhani, Y. Horie, eds.), part II, p. 751.

[3] E. Bar-on, et al: Int. J. Impact Engng. Vol. 27 (2002), p.509.

[4] D. Zhang, M.S. Wu, and R. Feng: Mechanics of Materials Vol. 37 (2005), p.95.

[5] G.I. Kanel: in Shock Compression of Condensed Matter (M.D. Furnish, M. Elert, T.P. Russel, eds), part II (2005), p. 870.

[6] R.C. Yu, G. Ruiz, and A. Pandolfi: Engng. Fracture Mech., Vol. 71 (2004), p. 897.

[7] A.S.Savinykh, S.V.Razorenov, and G.I. Kanel in Physics of Extreme States of Matter (V.E. Fortov ed.), Chernogolovka (2002), p. 77.

[8] E.G. Skripnyak, V.A. Skripnyak, and V.V. Skripnyak in Shock Compression of Condensed Matter, 2011. AIP Conf. Proc. 1426, (2012), p.1157.